High Energy Physics and Nuclear Physics

Volume 21, Number 2

# Incomplete-Fusion-Fragmentation Model and Nuclear Liquid-Gas Phase Transition

Wang Hui, Zheng Yuming, Sa Benhao, and Zhang Xiaoze

(China Institute of Atomic Energy, Beijing, China)

**The incomplete-fusion-fragmentation model is used to analyze the fragmentation of the projectile remnant in the 600 MeV/u Au+Au reaction. The theoretical results of the mass number, the excitation energy, and the thermodynamic temperature of the projectile remnant agree well with experimental data. The backbending structure in the curve of temperature as a function of the excitation energy per nucleon, i.e., the evidence of liquid-gas phase transition, is reproduced and related to the decay mode transformation from the dominance of the multifragmentation mode to the vaporization mode.**

**Key words: ALADIN multifragmentation data, projectile remnant, decay modes, thermodynamical temperature, liquid-gas phase transition.**

## 1. INTRODUCTION

In recent years the GSI-ALADIN group studied the fragmentation of the projectile remnant in the reactions of Au bombarding with C, Al, Cu, Au, and Pb targets at energies 100, 400, 600, and 1000 MeV/u [1-5]. The measurements include the change of the mean multiplicity of the intermediate-mass fragments (IMF), $\langle M_{\mathrm{IMF}} \rangle$ as a function of the sum of the fragment charges, $Z_{\mathrm{bound}}$, for $3 \leq Z \leq 30$. Different decay modes of the projectile remnant ranging from the evaporation-like mode at large $Z_{\mathrm{bound}}$ to the complete projectile remnant fragmentation at small $Z_{\mathrm{bound}}$ are observed. Other correlations between the observables concerning the charge of fragments and $Z_{\mathrm{bound}}$, such as the average charge of

Received December 13, 1995. Supported by the National Natural Science Foundation of China.

the largest fragment $\langle Z_{max}\rangle$, the two-body asymmetries $a_{12}$ and $a_{23}$, the three-body asymmetry $a_{123}$, and the ratio of charge moments $\gamma_2$, the charge Dalitz plots and the Campi plot ($\ln\langle Z_{max}\rangle$ vs. $\ln\langle M_2/M_1\rangle$) are also given. These observed results are almost independent of the target size and the bombarding energies; this confirms forcefully the formation of the projectile remnant (hot nucleus) before its decay and the statistical properties of the decay of the hot nucleus. The ALADIN data have already been explained successfully by the statistical model, the hybrid dynamical-statistical model, the combination of dynamics and percolation calculations [4-11], and the incomplete-fusion-fragmentation model (IFFM) [12-17].

Recently the ALADIN/LAND group [18,19] has confirmed the evidence of the nuclear liquid gas phase transition in the study of the decay of the projectile remnant in the Au+Au reaction at 600 MeV/u. From the measured fragment mass and charge distributions the mass and charge numbers $A_0$ and $Z_0$, the excitation energy $E_0$, and the temperature $T_{HeLi}$ of the projectile remnant are extracted. The experimental curve of temperature $T$ vs. the excitation energy per nucleon $\langle E_0\rangle$ / $\langle A_0\rangle$ can be divided distinctly into three sections: first, $T_{HeLi}$ increases with the increase of $\langle E_0\rangle$ / $\langle A_0\rangle$ due to the behavior of the Fermi liquid when $\langle E_0\rangle$ / $\langle A_0\rangle$ < 3 MeV; second, $T_{HeLi}$ keeps an approximate constant value of 4.5 — 6 MeV within the $\langle E_0\rangle$ / $\langle A_0\rangle$ range of 3 to 10 MeV per nucleon; third, $T_{HeLi}$ increases steadily with a slope parameter of 2/3 like the classical Fermi gas. This evidence of the liquid-gas phase transition has not been explained theoretically yet.

In this paper the IFFM is used to analyze the decay of the projectile remnant in the 600 MeV/u Au+Au reaction. After fitting the correlation of $\langle M_{IFM}\rangle$ vs. $\langle Z_{bound}\rangle$ by adjusting slightly the model parameter for the excitation energy, not only the theoretical results of the mass number, excitation energy, and thermodynamical temperature of the projectile remnant agree quite well with data, but also the backbending structure in the caloric curve of temperature vs. the excitation energy per nucleon, i.e., the evidence of the liquid-gas phase transition, is reproduced nicely. The liquid-gas phase transition and the decay mode transformations are related.

## 2. MODEL DESCRIPTION

The IFFM [12-17] is a hybrid dynamic-statistical model. In this model the intermediate-energy nucleus-nucleus collision is described simply as a two-step process of the formation and the decay (fragmentation) of hot nuclei. The formation of the hot nucleus is depicted as a dynamic process (incomplete fusion process) and the decay of the hot nucleus is regarded as a statistic process.

It is assumed that the target nucleons and the projectile nucleons inside the overlapping region between the target and projectile nuclei under a given impact parameter form the target remnant (one of the hot nucleus). The projectile remnant (another hot nucleus) is composed of projectile nucleons outside the overlapping region. They are used to describe the nuclear reaction products and their various physical distributions in the fragmentation of the target remnant and the projectile remnant, respectively.

The number of projectile nucleons inside the overlapping region between the projectile and target nuclei at impact parameter $b$ reads

$$N_P(b)=\rho_0\int \mathrm{d}V\theta\{R_P-[x^2+(b-y)^2+z^2]^{1/2}\}\theta\{R_T-(x^2+y^2)^{1/2}\}, \tag{1}$$

where $\rho_0 = 0.16\ \mathrm{fm}^{-3}$ refers to the normal nuclear density, and $\theta(x)$ stands for the step function. Thus one can obtain the mass numbers of the projectile remnant and target remnant, $A_P$ and $A_T$, respectively. If one assumes that the ratio of the charge to mass of the projectile remnant is equal to the corresponding ones of the projectile nucleus, one may obtain the charge numbers of the projectile and the target remnants $Z_P$ and $Z_T$, respectively.

Assuming that the projectile spectator nucleons escape as a whole (projectile remnant) with beam velocity in the incomplete fusion stage, the reaction energy $Q$ can be calculated from the mass conservation. From the energy and the momentum conservation, one can calculate the available energy deposited in the hot compound nuclear system (target and projectile remnants)

$$E_{\text{avai}} = \frac{N_{\text{P}}}{A_{\text{P}}^0} \frac{A_{\text{T}}^0}{A_{\text{T}}^0 + N_{\text{P}}} E_{\text{in}} + Q, \tag{2}$$

and the energy deposited in the projectile remnant

$$E_{\text{P}} = f_{\text{P}} \frac{A_{\text{P}}}{A_{\text{P}} + A_{\text{T}}} E_{\text{avai}} . \tag{3}$$

The energy deposited in the target remnant can be calculated similarly. The total excitation energy of the projectile remnant reads

$$E_{\text{P}}^* = C_{\text{P}} \times E_{\text{P}} \tag{4}$$

and the corresponding excitation energy per nucleon is $\varepsilon_{\text{P}}^* = E_{\text{P}}^* / A_{\text{P}}$. In the above formulas, $A_{\text{P}}^0$ and $A_{\text{T}}^0$ stand for the mass numbers of the projectile and target nuclei, respectively; $E_{\text{in}}$ refers to the incident energy, $f_{\text{P}}$ is a weight parameter characterizing the portion of the available reaction energy taken by the nucleons of the projectile remnant, $C_{\text{P}}$ is a fractional factor describing the part of energy $E_{\text{P}}$ which turns into excitation energy. The other part is consumed in the process approaching to a thermal equilibrium (freeze-out), such as in the pre-equilibrium emission, the expansion flow, etc. The fractional factor $C_{\text{f}}^{\text{P}} = f_{\text{P}} \times C_{\text{P}}$ is regarded as a model parameter.

The hot nucleus then decays according to the statistic law, i.e., its decay is described by the simultaneous multifragmentation model (the Berlin-Beijing model) [20,21]. In the Berlin-Beijing model (BBM) it is assumed that the hot nucleons disassembles promptly into a configuration described by a set of variables $\{N_{\text{c}}, N_{\text{N}}, \{A_i, Z_i\}_{i=1}^{N_{\text{c}}}, \{r_i\}_1^{N_{\text{c}}}, \{p_i\}_1^{N_{\text{c}}}, \{\varepsilon_i\}_1^{N_{\text{c}}}, \{r_j\}_1^{N_{\text{n}}}, \{p_j\}_1^{N_{\text{n}}}\}$. Here $N_{\text{c}}$ refers to the number of the charged fragments including protons. $N_{\text{n}}$ stands for the number of the prompt and evaporated neutrons. $\{A_i, Z_i\}_{i=1}^{N_{\text{c}}}$, $\{r_i\}_1^{N_{\text{c}}}$, $\{p_i\}_1^{N_{\text{c}}}$ and $\{\varepsilon_i\}_1^{N_{\text{c}}}$ are the mass and charge numbers, the position, momentum, and internal excitation energy of the charged fragments, respectively. $\{r_i\}_1^{N_{\text{n}}}$ and $\{p_i\}_1^{N_{\text{n}}}$ are the position and momentum of the neutron. The configurations allowed by the mass, charge, momentum, and energy conservation are assumed to have a canonical distribution or microcanonical ensemble. By means of the Monte Carlo method and the corresponding Metropolis technique a large number of the allowed configurations (say, $10^7$) are generated and the physical observable can be calculated as a statistical average and as an average over impact parameter if necessary. The results can be compared to the data.

## 3. RESULTS AND DISCUSSIONS

Figure 1 shows the mean multiplicity of the IMF, $\langle M_{\text{IFM}} \rangle$, as a function of $\langle Z_{\text{bound}} \rangle$ in the disassembly of the projectile remnant in the 600 MeV/u Au+Au reaction. The results of the IFFM are well consistent with the ALADIN data [18,19]. One can see from this figure that $\langle M_{\text{IFM}} \rangle$ increases first with the decreasing of $\langle Z_{\text{bound}} \rangle$, and then decreases after $\langle Z_{\text{bound}} \rangle$ approaches a maximum value of ~40. That reflects the decay mode transformation processes of the hot nucleus from the dominant pseudo-evaporation mode to the multifragmentation mode and then to the vaporization mode dominance [22,24] with the change in the violence of collisions.

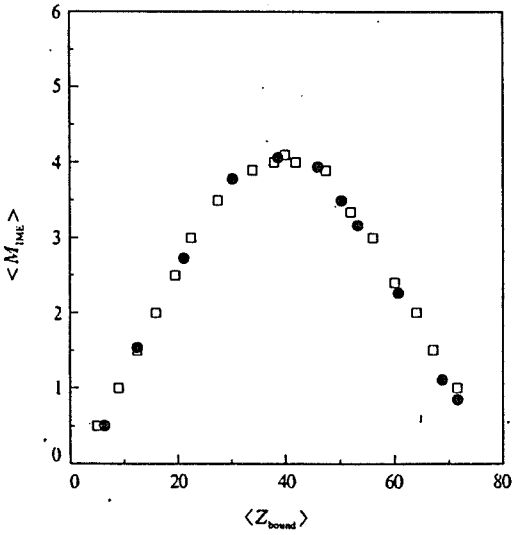


**Fig. 1**

The mean multiplicity of intermediate mass fragments, $\langle M_{IFM} \rangle$, as a function of $Z_{bound}$ in the 600 MeV/u Au+Au reaction.
$Z_{bound}$ is the sum of the charges of fragments with charge number $Z_f \geq 2$.
□ stand for the ALADIN data and • are the results of IFFM.

In the calculation the model parameter $C_f^P$ ($\approx 0.10 \times 0.70 = 0.07$) is adjusted to fit the maximum value of $\langle M_{IFM} \rangle$ in Fig. 1. Since for $\langle Z_{bound} \rangle < 20$ the projectile remnant is very small, the corresponding fluctuation of the excitation energy per nucleon is rather large. Thus when $\langle Z_{bound} \rangle < 20$ we increase the mean excitation energy per nucleon gradually according to the trend of the experimental curve of $\langle E_P \rangle / \langle A_P \rangle$ vs. $\langle Z_{bound} \rangle$, instead of approaching to a saturation value as done in Refs. [4,6-12], and [17].

The mass number of the projectile remnant, $\langle A_P \rangle$, as a function of $\langle Z_{bound} \rangle$ is given in Fig. 2 for a given interval of $Z_{max}$ (the charge of the largest fragment). The agreement between the ALADIN data and results of the IFFM is reasonably good except for the region of very small $\langle Z_{bound} \rangle$ where the calculated results of the IFFM are slightly smaller. Both of the theoretical and experimental results show that $\langle A_P \rangle$ decreases linearly with the decrease of $\langle Z_{bound} \rangle$ and is independent of the $Z_{max}$ bin.

Figure 3 gives the mean excitation energy per nucleon of the projectile remnant, $\langle E_P \rangle / \langle A_P \rangle$, as a function of $\langle Z_{bound} \rangle$ for a given interval of $Z_{max}$. A laser value of $\langle E_P \rangle / \langle A_P \rangle$ corresponds to a smaller $Z_{max}$, i.e., corresponds to a disassembly with more light fragments for a given mass number of the hot nucleus.

The experimental mean excitation energy is calculated according to the suggestion of Campi *et al.* [18,25], i.e., the mean excitation energy $\langle E_P \rangle$ is deducted from the energy conservation for each event

$$\langle E_P \rangle = \left( \langle \sum_i m_i \rangle + \langle \sum_i K_i \rangle \right) - (\langle m_0 \rangle + \langle K_0 \rangle), \tag{5}$$

where $m_i$ and $K_i$ are the mass and kinetic energy of the $i$-th fragment, respectively. $m_P$ and $K_P$ are the mass and kinetic energy of the projectile remnant will mass number $A_P$ and charge number $Z_P$. It should be pointed out that $\langle E_P \rangle$ corresponds to the available reaction energy of the projectile remnant

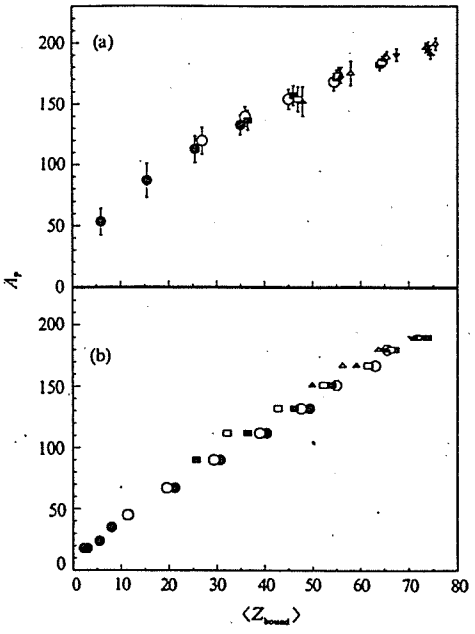


**Fig. 2**

The mass number of the projectile remnant $\langle A_P \rangle$ for a given $Z_{max}$ bin as a function of $Z_{bound}$ in the 600 MeV/u Au+Au reaction. (a) The ALADIN data and (b) the results of IFFM. The $Z_{max}$ bins are ●: 2—10, ○: 11—20, ■: 21—30, □: 31—40, ▲: 41—50, △: 51—60, ▼: 61—70, and ◇: 71—80.

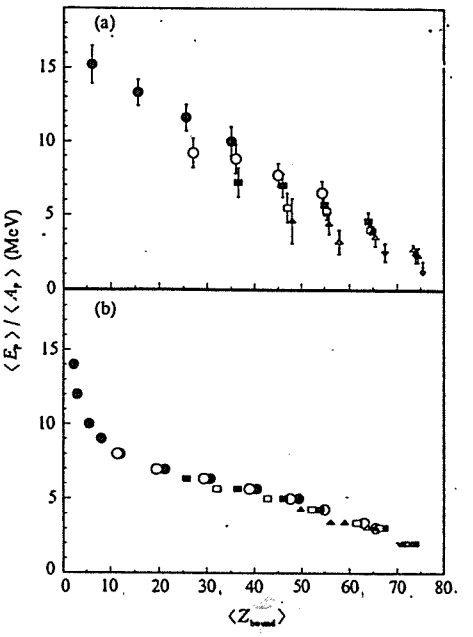


**Fig. 3**

The excitation energy per nucleon of the projectile remnant for a given $Z_{max}$ bin as a function of $Z_{bound}$ in the 600 MeV/u Au+Au reaction.

See the captions of Fig. 2 for the detail of the labels.

in the IFFM. Only part of $\langle E_P \rangle$ becomes the real excitation energy and the other part is consumed in the processes of the pre-equilibrium emission, the expansion flow, etc., as mentioned by Campi *et al.* in their paper [25]. This might be the reason why the theoretical results are systematically lower than the experimental ones and the deviation between the data and theoretical results increases with the decrease of $\langle Z_{bound} \rangle$ due to the increase of the energy consumed in the pre-equilibrium emission and the expansion flow.

The plot of the thermodynamic temperature $T$ vs. the excitation energy per nucleon $\langle E_P \rangle$ / $\langle A_P \rangle$ for the projectile remnant in the 600 MeV/u Au+Au reaction is shown in Fig. 4(b). Here,

$$T = \left\langle \frac{2E_0'}{3(N_c + N_v) - 5} \right\rangle , \tag{6}$$

where $N_v$ is the number of the prompt neutrons, $E_0'$ is the total kinetic energy of the fragments and prompt neutrons. The results of the IFFM (full circles) agree reasonably with the ALADIN data (open circles). According to the point of view mentioned above, the experimental plateau should be a little bit narrower if the excitation energy is smaller. Thus the agreement between the experiment and theory could become better. This temperature plateau is regarded as the evidence of the liquid-gas phase transition.

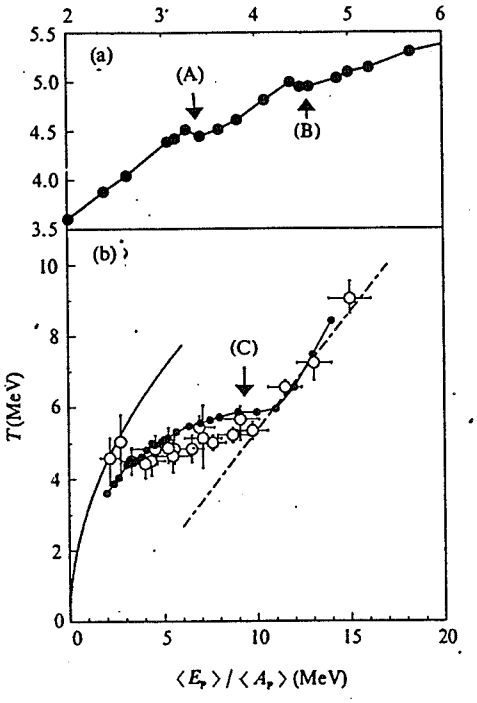


**Fig. 4**

Thermodynamic temperature $T$ as a function of the excitation energy per nucleon $\langle E_P \rangle$ / $\langle A_P \rangle$ for the projectile remnant in the 600 MeV/u Au+Au reaction.

(a) An amplification of a part of IFFM results in (b). (b) Comparison between ALADIN data and results of IFFM. • refer to the results of IFFM; o stand for the ALADIN data. See text for details.

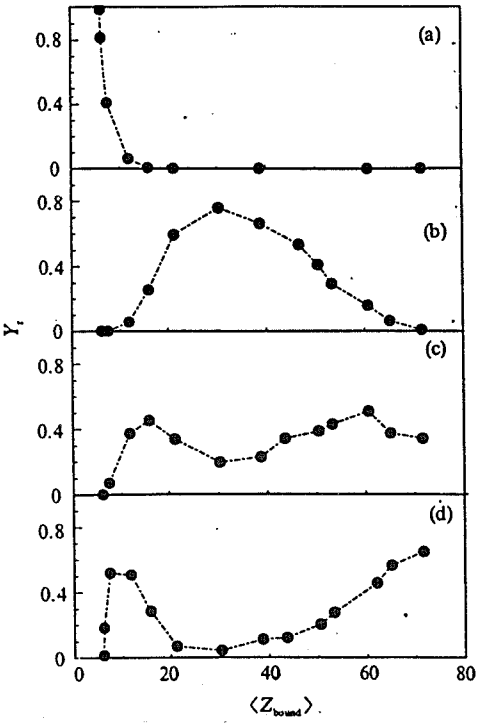


**Fig. 5**

The relative yield of decay mode as a function of $\langle Z_{bound} \rangle$ for the projectile remnant in the 600 MeV/u Au+Au reaction.

(a) the vaporization mode, (b) the multifragmentation mode, (c) the pseudofission mode, and (d) the pseudo-evaporation mode.

Figure 4(a) is an amplification of a part of the IFFM results in Fig. 4(b). One sees clearly from Fig. 4 that there are backbending structures (A), (B), and (C) which correspond to different decay mode transformations: (A) E (evaporation mode) → E + F (pseudofission mode); (B) E + F → M (multifragmentation mode); (C) M, F, E → V (vaporization mode). Since the ALADIN data are the charge distributions of fragments, here the decay mode is defined according to the charge number of the referential fragment $Z_r$

$$Z_r = \frac{Z_h}{C} \tag{7}$$

In the above equation, $Z_h$ refers to the charge number of the hot nucleus and the constant $C$ is selected to be nearly equal to 10. The E mode is then defined as the event that only one fragment has the charge number $Z_f \geq Z_r$ and the remaining fragments have smaller $Z_f$. The F mode indicates the event with only two big fragments $Z_{f1}$, $Z_{f2} \geq Z_r$. The M mode is the event with at least three fragments $Z_{f1}$, $Z_{f2}$, $Z_{f3} \geq Z_r$. The V mode stands for the event which is only composed of the protons, neutrons, alpha particles, and light fragments with $Z_f \leq 2$.

From Fig. 5 one sees more clearly the competition and transformation of the above decay modes of the projectile remnant. When $\langle Z_{bound} \rangle$ is very large, the E decay mode is dominant, the F mode is small, and no M and V modes exist there at all. With the decrease of $\langle Z_{bound} \rangle$, the events of the E mode decrease, the F mode increases first and then reaches a maximum value, the M mode appears and rises, but there is still no V mode. Thus the transformation of the E → E + F mode emerges here. With $\langle Z_{bound} \rangle$ decreasing, the E mode decreases continuously, the F mode turns to decrease, the M mode increases rapidly, and there is still no V mode. Here, one sees the transformation of the E + M → M mode. With a further decrease of $\langle Z_{bound} \rangle$, the M mode decreases quickly, the E and F modes increase to maximum values and then drop down rapidly. In the meantime the M mode increases dramatically and becomes dominant. Thus the transformation of M, F, E → V mode appears. The decay mode transformations mentioned above correspond to the temperature backbending structures indicated in Fig. 4, respectively.

## REFERENCES


[1] M.B. Tsang *et al.*, *Phys. Rev. Lett.*, **71**(1993), p. 1502.
[2] C.A. Ogilvie *et al.*, *Phys. Rev. Lett.*, **67**(1991), p. 1214.
[3] J. Hubele *et al.*, *Z. Phys.*, **A340**(1991), p. 263; J. Hubele *et al.*, *Phys. Rev.*, **C46**(1992), R1577.
[4] P. Kreutz *et al.*, *Nucl. Phys.*, **A556**(1993), p. 672.
[5] W. Trautmann *et al.*, GSI Preprint 93-76 (1993); also GSI 05-94.
[6] A.S. Botvina and I.N. Mishustin, *Phys. Lett.*, **B294**(1992), p. 23; A.S. Botvina *et al.*, *Nucl. Phys.*, **A584**(1995), p. 737.
[7] H.W. Barz, W. Bauer, J.P. Bondorf *et al.*, *Nucl. Phys.*, **A561**(1993), p. 466.
[8] Bao-An Li, A.R. DeAngelis and D.H.E. Gross, *Phys. Lett.*, **B303**(1993), p. 225.
[9] J. Pochodzalla *et al.*, *Nucl. Phys.*, **A583**(1995), p. 553c.
[10] Y.M. Zheng, J. Richert and P. Wagner, *Chinese J. Nucl. Phys.*, **17**(1995), p. 215.
[11] Y.M. Zheng, J. Richert and P. Wagner, *J. Phys.*, **G22**(1996), p. 505.
[12] Zheng Yuming, Wang Fei, Sa Benhao *et al.*, *Phys. Rev.*, **C53**(1996), p. 1868.
[13] Sa Benhao, Zheng Yuming and Zhang Xiaoze, *Phys. Rev.*, **C40**(1989), p. 2680.
[14] Chih Tahai, Sa Benhao, Zhang Xiaoze *et al.*, *Phys. Rev.*, **C42**(1990), p. 2187.
[15] W.X. Li, T.Y. Sun, T.H. Chih *et al.*, *Phys. Rev.*, **C48**(1993), p. 628.
[16] Zheng Yuming, Chih Tahai, Li Wenxin *et al.*, *Chinese J. Nucl. Phys.*, **14**(1992), p. 116.
[17] Wang Fei *et al.*, *High Energy Physics and Nuclear Physics* (Chinese Edition), **20**(1996), p. 644; Wang Fei *et al.*, *High Energy Physics and Nuclear Physics* (Chinese Edition), **20**(1996), p. 729.
[18] J. Pochodzalla *et al.*, *Phys. Rev. Lett.*, **75**(1995), p. 1040.
[19] W.F.J. Müller *et al.*, Report No. GSI-Nachrichten-03-95, 1995.
[20] Zhang Xiaoze, D.H.E. Gross, Xu Shuyan *et al.*, *Nucl. Phys.*, **A461**(1987), p. 641; p. 668.
[21] Sa Benhao and D.H.E. Gross, *Nucl. Phys.*, **A437**(1985), p. 643.
[22] Zheng Yuming, H. Massmann, Xu Shuyan *et al.*, *Phys. Lett.*, **B194**(1987), p. 183.
[23] D.H.E. Gross, Yuming Zheng and H. Massmann, *Phys. Lett.*, **B200**(1988), p. 397.
[24] Sa Benhao, Zheng Yuming and Zhang Xiaoze, *Int. J. Mod. Phys.*, **A5**(1990), p. 843.
[25] X. Campi, H. Krivine and E. Plagnol, *Phys. Rev.*, **C50**(1994), R2680.